

RESEARCH ARTICLE

Change in the central control of the bladder function of rats with focal cerebral infarction induced by photochemically-induced thrombosis

Yuya Ota^{1*}, Yasue Kubota^{1,2*}, Yuji Hotta³, Mami Matsumoto⁴, Nayuka Matsuyama¹, Taiki Kato¹, Takashi Hamakawa¹, Tomoya Kataoka⁵, Kazunori Kimura^{3,5}, Kazunobu Sawamoto^{4,6}, Takahiro Yasui¹

1 Department of Nephro-Urology, Graduate School of Medical Sciences and Medical School, Nagoya City University, Nagoya, Japan, **2** Department of Clinical Physiology, Nagoya City University Graduate School of Nursing, Nagoya, Japan, **3** Department of Hospital Pharmacy, Graduate School of Pharmaceutical Sciences, Nagoya City University, Nagoya, Japan, **4** Department of Developmental and Regenerative Neurobiology, Institute of Brain Science, Nagoya City University Graduate School of Medical Sciences, Nagoya, Japan, **5** Department of Clinical Pharmaceutics, Nagoya City University, Graduate School of Medical Sciences and Medical School, Nagoya, Japan, **6** Division of Neural Development and Regeneration, National Institute for Physiological Sciences, Okazaki, Japan

* y-ota@med.nagoya-cu.ac.jp (YO); yasuekbt@med.nagoya-cu.ac.jp (YK)



OPEN ACCESS

Citation: Ota Y, Kubota Y, Hotta Y, Matsumoto M, Matsuyama N, Kato T, et al. (2021) Change in the central control of the bladder function of rats with focal cerebral infarction induced by photochemically-induced thrombosis. PLoS ONE 16(11): e0255200. <https://doi.org/10.1371/journal.pone.0255200>

Editor: Peter F.W.M. Rosier, University Medical Center Utrecht, NETHERLANDS

Received: July 9, 2021

Accepted: October 15, 2021

Published: November 9, 2021

Copyright: © 2021 Ota et al. This is an open access article distributed under the terms of the [Creative Commons Attribution License](https://creativecommons.org/licenses/by/4.0/), which permits unrestricted use, distribution, and reproduction in any medium, provided the original author and source are credited.

Data Availability Statement: All relevant data are within the manuscript and its [Supporting Information](#) files.

Funding: This work was supported by GSK Japan Research Grant 2019 (<https://jp.gsk.com/jp/research/glaxosmithkline-research-grant-2019/>) and a grant awarded by the Japan Society for the Promotion of Science (<https://www.jsps.go.jp/j-grantsinaid/>), Grant Number 19k18568, all to Y.O..

Abstract

The photochemically-induced thrombosis (photothrombosis) method can create focal cerebral infarcts anywhere in the relatively superficial layers of the cerebrum; it is easy to implement and minimally invasive. Taking advantage of this versatility, we aimed to establish a new rat model of urinary frequency with focal cerebral infarction, which was characterized by its simplicity, nonlethal nature, and high reproducibility. The prefrontal cortex and the anterior cingulate cortex, which are involved in lower urinary tract control, were targeted for focal cerebral infarction, and urinary parameters were measured by cystometrogram. Cystometric analysis indicated that micturition intervals significantly shortened in photothrombosis-treated rats compared with those in the sham operative group on Days 1 and 7 ($P < 0.01$), but prolonged after 14 days, with no difference between the two groups. Immunopathological evaluation showed an accumulation of activated microglia, followed by an increase in reactive astrocytes at the peri-infarct zone after photothrombotic stroke. Throughout this study, all postphotothrombosis rats showed cerebral infarction in the prefrontal cortex and anterior cingulate cortex; there were no cases of rats with fatal cerebral infarction. This model corresponded to the clinical presentation, in that the micturition status changed after stroke. In conclusion, this novel model combining nonlethality and high reproducibility may be a suitable model of urinary frequency after focal cerebral infarction.

Competing interests: The authors have declared that no competing interests exist.

Introduction

Cerebral infarction is associated with a high incidence of lower urinary tract symptoms (LUTS), particularly urinary bladder overactivity, which reduces a patient's quality of life [1,2]. Therapies that target bladder receptors, such as anticholinergics and beta-3 adrenaline receptor stimulants, have been used to treat LUTS caused by stroke, but they are not sufficiently effective [3,4]. Currently, there is no established LUTS treatment that targets the central nervous system. We believe that one of the reasons for the lack of development of treatments for the central nervous system is the lack of animal models.

Middle cerebral artery occlusion (MCAO) rats have generally been used as a model for bladder overactivity caused by cerebral infarction [5,6]. However, they have the disadvantages of variability in the infarct volume and a high mortality rate due to the large infarct area and local traumatic effect [5,7,8]. Furthermore, creating an MCAO rat model is surgically demanding [9].

Establishing a simple and reproducible animal model of LUTS caused by cerebral infarction is needed to solve these issues. Therefore, we focused on applying photochemically-induced thrombosis (photothrombosis) as a method for creating focal cerebral infarcts [10]. The principle of arterial occlusion achieved by photothrombosis is the formation of a stable thrombus that consists solely of aggregated platelets in response to endothelial peroxidative damage in laser irradiated areas [11]. Depending on where the light is applied, photothrombotic reaction can create focal cerebral infarcts anywhere in the relatively superficial layers of the cerebrum. Although photothrombosis has been used in various brain experiments [12,13], it has never been applied for studying urinary function.

The periaqueductal gray (PAG) region receives sacral afferents related to bladder filling and transmits efferent signals to the sacral spinal cord or bladder via the pontine micturition center (PMC) [14]. Previous reports have shown that the prefrontal cortex (PFC) and the anterior cingulate cortex (ACC) exert supra-inhibitory control of these voiding reflexes both experimentally and clinically [15–18], indicating that urination can be initiated and inhibited voluntarily by PFC and ACC. In other words, a cerebral infarction of PFC and ACC may impair urinary control and lead to a subsequent increase in urinary frequency. In the acute stage of cerebral infarction, a region called the penumbra develops around the center of the ischemic foci, and salvaging this region is one of the important factors that can aid in early recovery from stroke [19,20]. However, to the best of our knowledge, there are no reports on the assessment of the ischemic area in animal models of frequent urination after stroke.

Our aim was to establish a new rat model of urinary frequency, with focal cerebral infarction in PFC and ACC induced by photothrombosis, which is easy to perform and minimally invasive, and to observe histopathological changes in the brain.

Materials and methods

Experimental design and animals

All experimental protocols were approved by the Animal Care Committee of Nagoya City University Graduate School of Medical Sciences, Nagoya, Japan (No. H30M-57). The study design is shown in Fig 1. A total of 90 11-week-old female Wistar-ST rats were purchased from SLC Inc. (Shizuoka, Japan). Ten rats were allocated for the evaluation of the infarct area and volume, in a small pilot study, and 40 rats each were assigned to a sham group and a photothrombosis-treated group. Neurological evaluation, cystometric measurements, and immunohistochemical evaluation of the brain were performed preoperatively and on postoperative Days 1, 7, 14, and 28, (n = 8). We did not correct cystometrograms data for some rats because

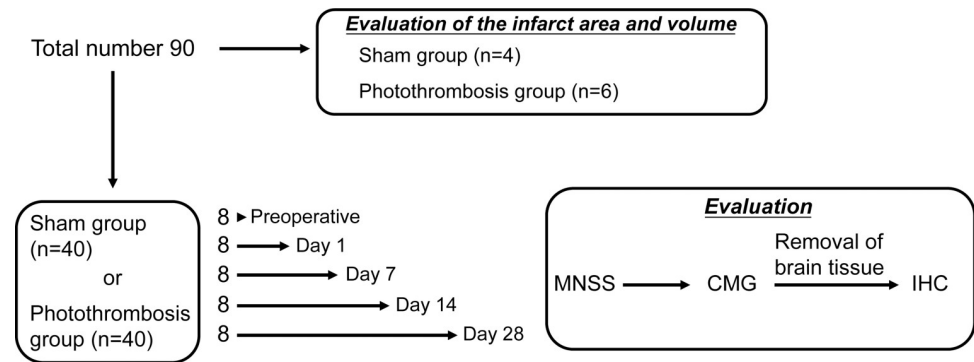


Fig 1. Study design.

<https://doi.org/10.1371/journal.pone.0255200.g001>

of cannula withdrawal during measurement. Thus, the final preoperative numbers were: $n = 36$ (Preoperative, $n = 8$; Day 1, $n = 8$; Day 7, $n = 6$; Day 14, $n = 7$; Day 28, $n = 7$) in the sham group, and $n = 38$ (Preoperative, $n = 8$; Day 1, $n = 7$; Day 7, $n = 8$; Day 14, $n = 7$; Day 28, $n = 8$) in the photothrombosis group. The rats were maintained at $21 \pm 2^\circ\text{C}$ with a 12-h light-dark cycle and were allowed free access to water and provided a standard laboratory diet. The body temperature of the rats was maintained at $37 \pm 0.5^\circ\text{C}$ using a controlled heating plate during experiments. All efforts were made to minimize the number of animals used and their suffering.

Photothrombosis

We used a modified version of the photothrombosis technique described by Watson to induce cerebral infarction [10]. The rats were subjected to 4% isoflurane inhalation for induction and 1.5%–2.0% isoflurane for the maintenance of anesthesia. The scalp was incised to expose the skull surface and cleaned to reveal bregma and the target area for irradiation (S1A Fig). For illumination, a fiber optic cable delivering a light source of 8 mm in diameter (MSG6-1100S, Moritex, Saitama, Japan) was placed stereotactically onto the skull 1 mm anterior to the bregma on the midline (S1B Fig). Cerebral infarction was induced by activation of photosensitive Rose Bengal dye (30 mg/kg, 330000-1G; Sigma-Aldrich, St. Louis, MO, USA) in 0.9% NaCl solution. Two minutes prior to laser irradiation, Rose Bengal was injected through the caudal vein. The skull was illuminated for 30 min (wavelength 533 nm; 150 mW, MHAA-100W-100V, Moritex). Sham-operated rats received normal saline instead of Rose Bengal solution. After laser irradiation, the scalps were sutured, and the animals were allowed to recover in their home cages.

Assessment of infarction area and volume

It is known that 2,3,5-triphenyl tetrazolium chloride (TTC) (T8877, Sigma-Aldrich) staining allows for rapid assessment of the infarcted area [21]. This TTC staining can be used only in the first few days after stroke onset due to the action of mitochondrial enzyme systems [22]. Therefore, 1 day after photothrombosis, TTC staining was used to assess the area of cerebral infarction. The rats were euthanized in a chamber filled with carbon dioxide. Following sacrifice, the brains were removed from the skull and stored at -20°C for 10 min. The area of PFC and ACC is located 0.4 mm lateral to the midline in a sagittal section, according to the stereotactic section map designed by C. Watson and G. Paxinos [23]. Hence, the cerebral hemispheres were cut into sagittal slices, each 2-mm thick, based on a distance of 0.4 mm from the

midline, and incubated in 4% TTC–PBS at 37°C for 30 min. The area of infarction in each slice was measured using a digital scanner and Image J software (version 1.52u; National Institutes of Health, Bethesda, MD, USA). We assumed that the infarct extended across the entire 2-mm thickness. The volume of infarction in each animal was obtained as the product of average slice thickness and sum of infarction areas in all brain slices examined (infarct volume = area of infarct [mm^2] \times thickness [2 mm]) according to previously described methods [24].

Neurological evaluation

The modified neurological severity score (mNSS) was used to evaluate neurobehavioral functions [25]. The mNSS includes motor, sensory, reflex, and balance tests. Neurological function was graded on a scale of 0–18 (normal score, 0; maximal deficit score, 18). For severity, points are scored for the inability to perform a test or the lack of examined reflexes; thus, the higher the score, the greater the severity of the injury.

Cystometric investigations

After the neurological evaluation, all rats underwent cystometry according to methods described previously [26–28]. With inhalation anesthesia (4% isoflurane for induction and 1.5%–2.0% isoflurane for maintenance), the abdomens of the rats were opened through a midline incision, and the bladders were exposed. A polyethylene catheter tip (PE-50; inner diameter 0.5 mm, outer diameter 1.0 mm; Eastsidemed, Tokyo, Japan) was heated to make a collar that could fit tightly into the bladder. It was inserted into the bladder dome and sealed by a purse-string suture (5–0 silk suture) under a surgical microscope. After suturing, the bladder was filled with saline solution up to the leak point and a leak at the urethral meatus was observed, confirming that no leak had occurred at the suture site. The other end of the catheter was tunneled subcutaneously to the neck and connected to a syringe pump (U-802, Univentor, Zejtun, Malta) that was attached to a pressure transducer (MLT844; ADInstruments, Dunedin, New Zealand) to allow saline infusion. After suturing the abdominal skin, the rats were placed in a restraining cage (ICN-5; Tokyo Garasu Kikai, Tokyo, Japan) for the cystometrogram. Three hours after awakening from anesthesia, the bladders were filled with saline (room temperature) at 0.10 mL/min for 120 min, and intercontraction intervals (ICIs), baseline pressure (BP), micturition threshold pressure (TP, bladder pressure immediately prior to micturition), and maximum intravesical pressure (MP) were recorded for analysis. After the cystometrogram, the entire bladder was collected and weighed.

Brain preparation for histology

We used NeuN (1:500; mouse monoclonal, MAB377, Sigma-Aldrich) as a neural marker to assess the distribution of mature neurons. The area from which mature neurons had disappeared indicated the infarcted area. Anti-ionized calcium binding adaptor molecule 1 (Iba1) (1:2000; Rabbit polyclonal, 013–27691, Wako, Osaka, Japan) and anti-gial fibrillary acidic protein (GFAP) (1:2,000; mouse monoclonal, G3893, Sigma-Aldrich) were used to assess activated microglia and reactive astrocytes in ischemic regions, respectively. After cystometrogram, the rats were exsanguinated from their right auricle, following inhalant anesthesia using isoflurane, and transcardially perfused with 20 mL/body of 1% heparinized saline followed by 25 mL/body 10% formalin. The brains were removed, postfixed overnight for 24 additional h in 10% formalin at 4°C, and embedded in paraffin. All brain tissue were sectioned into 4- μm -thick sagittal cross-sections of PFC and ACC, which is located 0.4 mm lateral to the midline, as described above. The sections were deparaffinized in D-limonene and 100% ethanol (3 times

for 10 min) before rehydration in graded ethanol (90%, 80%, and 50%; 2 min each), followed by MilliQ-H₂O (5 min). Antigen retrieval was performed by heating the sections in 10 mM trisodium citrate dehydrate (pH 6) in Decloaking Chamber™ NxGen (Biocare Medical, Pacheco, CA, USA) at 95°C for 40 min before cooling at room temperature for 30 min. After blocking the endogenous peroxidase activity by methanol containing 3% H₂O₂, the brain slice tissues were incubated overnight at room temperature with antibody against NeuN. After washing in buffer, the sections were immunostained by the avidin–biotin peroxidase method using the Vectastain Elite Kit (PK-6102, Vector Laboratories, Burlingame, CA, USA) with 3--3-diaminobenzidine and hydrogen peroxide as the chromogen. For immunofluorescence staining, the brain slice tissues were incubated with anti-Iba1 and anti-GFAP overnight at 4°C, and incubated with goat anti-rabbit or goat anti-mouse secondary antibodies (1:2000; Zhongshan Goldbridge Biotechnology, Beijing, China) for 1 h at 25°C. For immunostaining and immunofluorescence analyses, BZ-X800 (Keyence, Osaka, Japan) was used to acquire digital images which were analyzed with a BZ-X800 Analyzer.

For quantification of immunofluorescence in the ischemic region, which is within 300 μm beneath the infarcted area, as indicated by NeuN staining, five microscopic images per rat were randomly captured at 40× objective using the microscope, according to previous reports [29]. In the sham group and preoperatively in the PT group, the images were taken randomly within the frontal lobe. The numbers of Iba1-, and GFAP-positive cells with identified same-threshold nuclei (4',6-diamidino-2-phenylindole [DAPI]-stained) were measured with a BZ-X800 Analyzer.

Statistical analysis

All statistical analyses were performed using the Statistical Package of Social Sciences 22 software[®] (SPSS; Chicago, IL, USA). The results are expressed as mean ± standard deviation (SD). Student's t-tests were used for comparison between the two groups. A two-way repeated measures analysis of variance (ANOVA) was used to perform multiple group comparisons, followed by Tukey's test for individual comparisons. The results were considered statistically significant at $P < 0.05$.

Results

Evaluation of infarction area and volume

As shown in Fig 2, the sagittal brain sections on Day 1 after photothrombosis revealed infarcted PFC and ACC lesions. All the rats in this study had similar areas of infarction (S2 Fig). No damage was observed in the brain stem, such as the PAG or PMC regions, in either group. The individual infarct volumes are detailed in the Supporting Information (S1 File). The mean infarction volume was $147.1 \pm 24.1 \text{ mm}^3$. No evidence of infarction was found in any of the sham rats.

General information

The body and bladder weights are shown in Table 1. There were no cases of rats with fatal cerebral infarction during the postoperative period. There were no statistical differences in body weight, bladder weight, or bladder body weight ratio (bladder weight/body weight) between the sham group and the photothrombosis group (PT group) at any time points.

Modified neurological severity score

Fig 3 shows the results of neurobehavioral assessments with the mNSS test for each rat. All of the individual data points are detailed in the Supporting Information (S2 File). Immediately

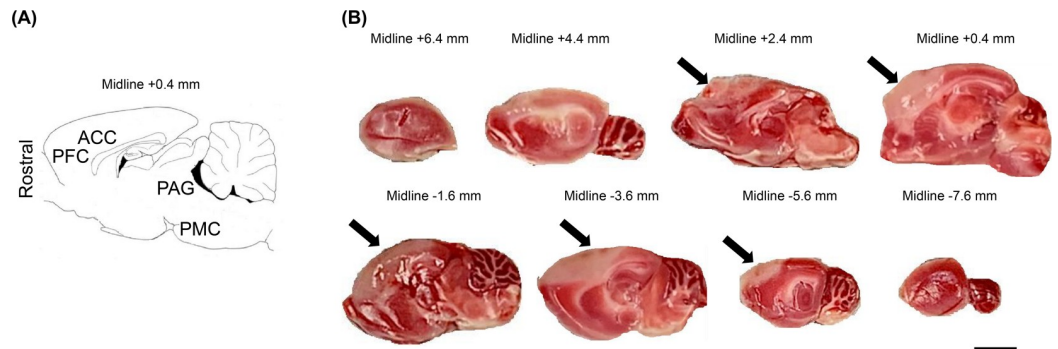


Fig 2. Diagrammatic representation of a sagittal section and triphenyl tetrazolium chloride (TTC)-stained brain images. A: Anterior cingulate cortex (ACC), prefrontal cortex (PFC), periaqueductal gray (PAG), and pontine micturition center (PMC) are present in the sagittal section 0.4 mm lateral to the midline identified according to the rat brain atlas of Paxinos and Watson. B: Examples of TTC-stained sagittal sections of rat brain on Day 1 after photothrombosis. Cerebral infarction was identified in PFC and ACC in the brains of all rats after photothrombosis. Arrows indicate unstained areas (areas of cerebral infarction). The distances from the midline are shown above each brain slice. Scale bars = 3 mm.

<https://doi.org/10.1371/journal.pone.0255200.g002>

after photothrombosis, the rats showed characteristic motor changes, with bilateral hind limbs flexed when suspended by the tail. Furthermore, rats with cerebral infarction from photothrombosis were observed to have balance disorders in the beam balance test (walking on a 3-cm beam); however, there were no sensory or reflex disturbances. There were no abnormal neurological findings in the sham group at all. Therefore, the mNSS was significantly higher in the PT group than in the sham group at all time points ($P < 0.01$). The neurological deficits tended to improve with time, but neurological damage was still present 28 days after the stroke.

Table 1. Body and bladder weights in the different groups.

	Sham group	Photothrombosis group	P-value
Body weight, g			
Preoperative	218.4 ± 7.3	219.3 ± 3.0	0.758
Day 1	214.9 ± 10.2	209.9 ± 6.2	0.208
Day 7	227.8 ± 10.1	221.9 ± 10.7	0.312
Day 14	242.4 ± 8.5	238.1 ± 6.3	0.303
Day 28	257.3 ± 4.2	252.4 ± 7.2	0.138
Bladder weight, mg			
Preoperative	151.6 ± 17.8	146.5 ± 13.8	0.531
Day 1	156.9 ± 20.7	154.1 ± 21.9	0.808
Day 7	164.0 ± 13.9	156.9 ± 19.3	0.459
Day 14	160.9 ± 17.4	163.4 ± 15.8	0.777
Day 28	166.1 ± 18.9	170.9 ± 20.0	0.647
Bladder body weight ratio ($\times 10^{-3}$)			
Preoperative	0.69 ± 0.08	0.67 ± 0.06	0.452
Day 1	0.73 ± 0.09	0.73 ± 0.10	0.919
Day 7	0.72 ± 0.05	0.71 ± 0.10	0.818
Day 14	0.66 ± 0.08	0.69 ± 0.07	0.599
Day 28	0.65 ± 0.03	0.68 ± 0.02	0.421

<https://doi.org/10.1371/journal.pone.0255200.t001>

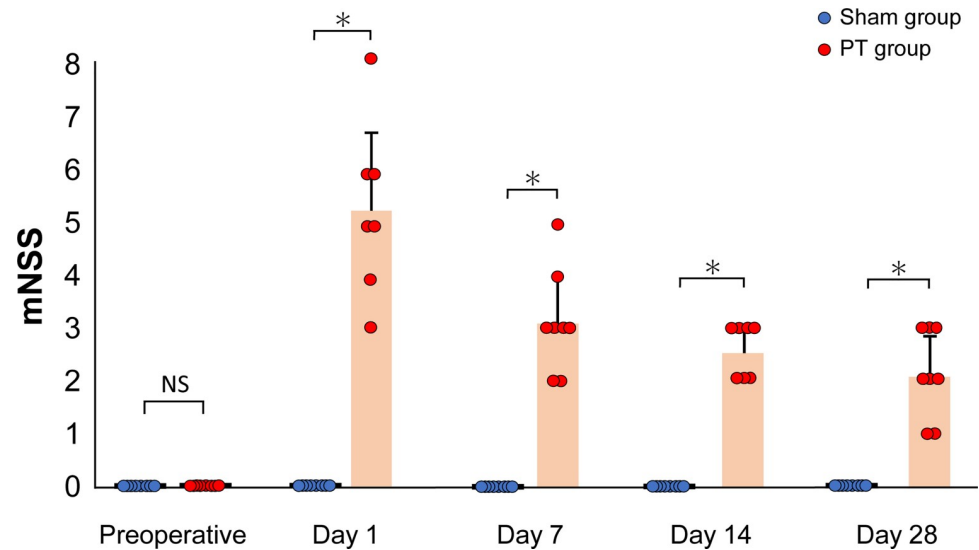


Fig 3. Time course of changes in the modified neurological severity score. Neurological function tests were performed on rats in the sham and photothrombosis (PT) groups at each time point. There were significant differences ($*P < 0.01$, Student's t-test) in the mNSS of each group. Values are represented in mean \pm SD.

<https://doi.org/10.1371/journal.pone.0255200.g003>

Assessment of the peri-infarct area

In the PT group, mature neurons were lost in the frontal lobe of the cerebral cortex and the ACC from Days 1 to 28, whereas they were present in the sham group and preoperatively in the PT group (Fig 4A). Immunofluorescence staining revealed positive cells for Iba1 and GFAP staining in the peri-infarct zone (Fig 4B). Quantitative immunofluorescence staining showed an increase in the number of Iba1- and GFAP-positive cells in the PT group compared with the sham group, from Day 1 to Day 28 and from Day 7 to Day 28 after photothrombosis, respectively (Fig 4C).

Cystometric investigations

The representative cystometric curves of each group are shown in Fig 5A. S3 File lists the raw cystometric data points used for preparing the figure graphs. The cystometric studies showed that ICIs in the PT group were significantly shorter than those in the sham group on Days 1 and 7 ($P < 0.01$) (Fig 5B). However, there was no significant difference between the sham and photothrombosis groups from Day 14 onwards. In the comparison within the PT group, the ICIs on Days 1 and 7 after photothrombosis were significantly shorter than the preoperative ICIs ($P < 0.01$). The ICIs on Days 14 and 28 after photothrombosis were significantly longer than those on Day 1 after photothrombosis ($P < 0.05$), and the ICIs on Day 28 after photothrombosis were significantly longer than those on Day 7 after photothrombosis ($P < 0.05$); therefore, the micturition status in the PT group worsened and subsequently improved. BP, TP, and MP did not differ between the two groups at any time point (Fig 5C–5E).

Discussion

In this study, we used a photothrombotic stroke method to induce focal infarcts in PFC and ACC, and we observed decreased ICIs on Days 1 and 7, according to the cystometric analysis. Furthermore, all rats survived after the operation. To the best of our knowledge, this is the first study in which photothrombosis has been applied to manipulate urinary function.

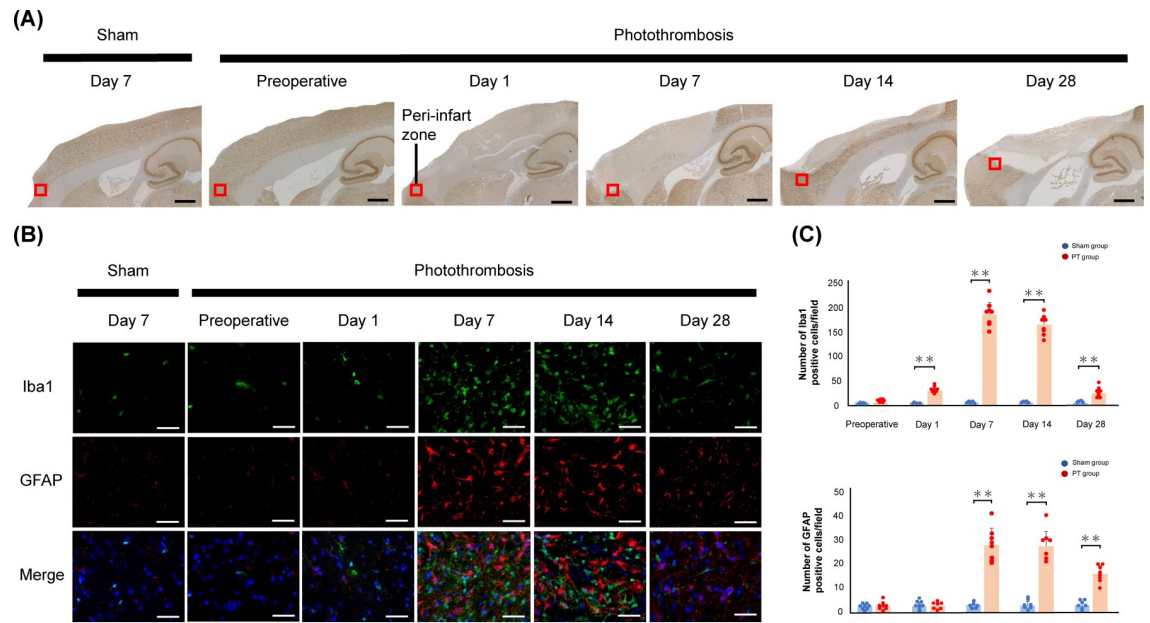


Fig 4. NeuN staining of sagittal sections and sustained activation of glial cells in ischemic regions. A: Schematic of a sagittal section (0.4 mm lateral to the midline) centered on the frontal lobe. The black square indicates the location of the peri-infarct zone. Scale bars: 1.5 mm. B: Immunofluorescence staining revealed activated microglia labeled with anti-ionized calcium binding adaptor molecule 1 (Iba1; green), reactive astrocytes labeled with anti-glial fibrillary acidic protein (GFAP; red), and nuclei labeled with 4',6-diamidino-2-phenylindole (DAPI; blue) in the ischemic regions after photothrombosis. Scale bar = 50 μ m. C: Quantification of Iba1-positive and GFAP-positive cells. Significant differences between the photothrombosis (PT) group and sham group are indicated by ** ($P < 0.01$, Student's t-test). Values are represented in mean \pm SD.

<https://doi.org/10.1371/journal.pone.0255200.g004>

The method of inducing a stroke in the cerebral cortex using photochemical reactions was developed by C. Watson in 1985 [10]. Photothrombosis has the advantage of reproducibility due to precise control of the size and location of the infarct, with similar characteristic inflammation and neurodegeneration to other established stroke models [11,30]. Hence, photothrombosis can target brain areas involved in lower urinary tract control, such as PFC and ACC for stroke lesions. Additional advantages of this photothrombotic model are the minimal surgical invasiveness required and the low mortality rate [31]. The greater the extent of the infarct, the more likely the urinary frequency will increase, but the incidence of other disorders will also increase, leading to increased mortality. We created a model of urinary frequency with only minimal periprocedural dysfunction, without suffering an infarction in the cerebellum, brainstem, or other limbic system, which is necessary to sustain vital functions. In this study, we used a light source with an 8-mm diameter for irradiation. If smaller light sources are used to create focal infarcts in the ACC, PFC, or other regions, such as the cerebellum, it would be possible to obtain more accurate localizations of which areas control micturition. Furthermore, a localized cerebral infarction can be created in any region by drilling the skull and inserting an optical fiber connected to a light source into the brain [32,33]. This photothrombosis method may be able to contribute to the understanding of neural control of urinary function by regulating the number and volume of the infarcted areas.

There was no difference in bladder weight or bladder to body weight ratio between the sham and PT groups, which is the same result as obtained in the MCAO model [6]. Furthermore, BP, TP, and MP did not differ between the two groups. This suggests that voiding is normal and the increase in urinary frequency is attributed to the dysfunction of the central nervous system. Yokoyama et al. reported that bladder overactivity after MCAO is the result of

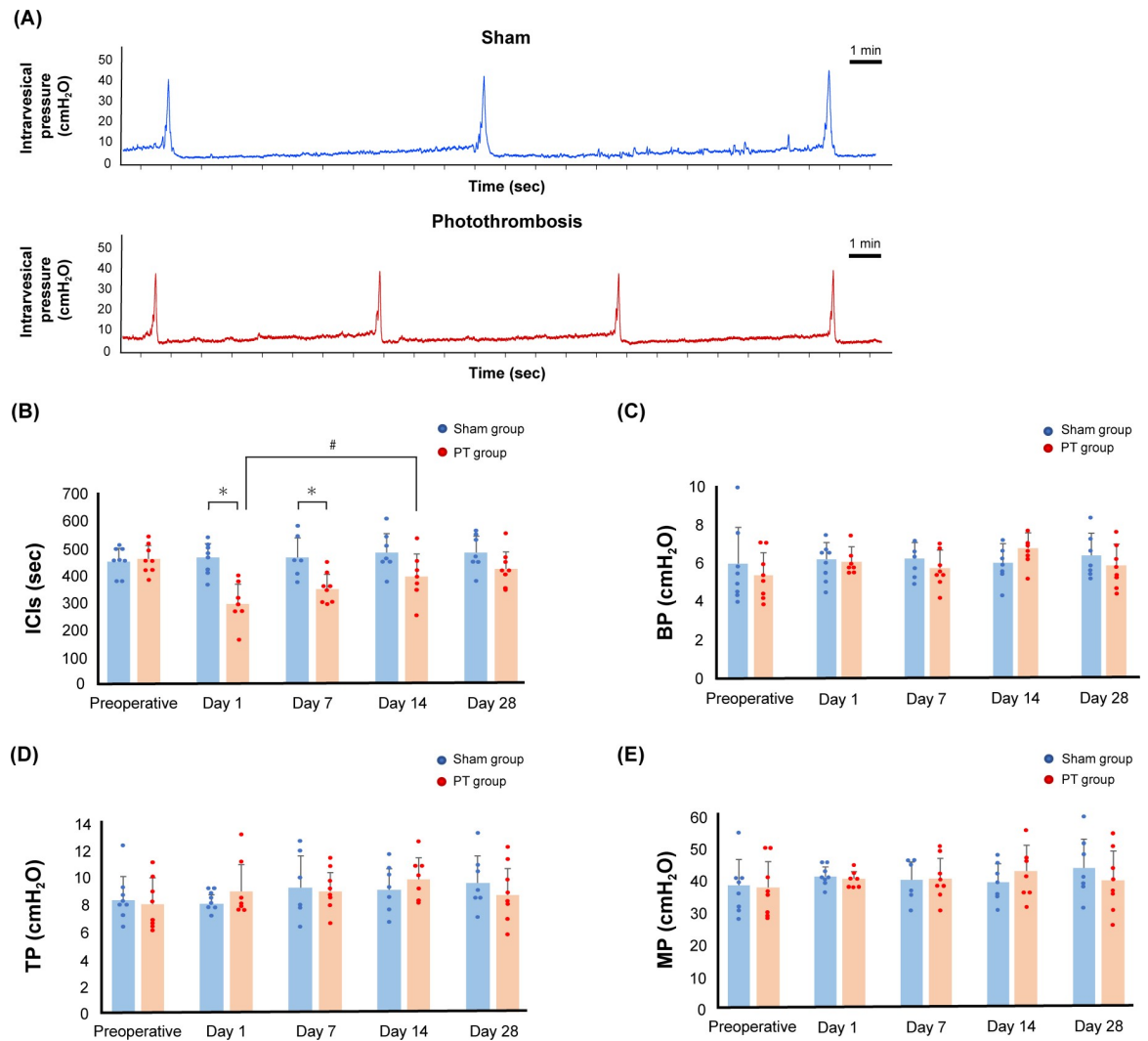


Fig 5. Cystometric study of the rats in the photothrombosis group compared with those in the sham group. A: The representative cystometric chart of each group on Day 1 after photothrombosis. B, C, D, and E: Time courses of the changes in intercontraction intervals (ICIs) (B), baseline pressure (BP) (C), micturition threshold pressure (TP, bladder pressure immediately prior to micturition) (D), and maximum intravesical pressure (MP) (E) of the rats in the sham group versus those in the photothrombosis (PT) group. Significant differences between ICIs in the sham and PT groups are indicated by # ($P < 0.01$, Student's t-test). In the PT group, significant differences in the ICIs on Days 1 and 7 compared with the preoperative ICIs are indicated by ** ($P < 0.01$, two-way ANOVA followed by Tukey's test for individual comparisons), and significant differences in ICIs on Days 14 and 28 compared with those on Day 1 are indicated by * ($P < 0.05$, two-way ANOVA followed by Tukey's test for individual comparisons). Significant differences in the ICIs on Day 28 compared with those on Day 7 are indicated by * ($P < 0.05$, two-way ANOVA followed by Tukey's test for individual comparisons). Values are represented in mean \pm SD.

<https://doi.org/10.1371/journal.pone.0255200.g005>

upregulation of the NMDA glutamatergic pathway from the forebrain, which promotes a sustained excitatory signal to the PMC [16,34]. Additionally, they state that bladder overactivity after MCAO persisted for 4 months. In the present study, rats with cerebral infarction induced by photothrombosis developed an increase in urinary frequency for a period of 1 week after ischemia, and showed improvement in urinary function by Day 14 after the onset of stroke. We believe that our animal model reflects the clinical presentation of stroke in humans as the voiding interval showed time-course changes after stroke. It has been clinically observed that urinary status changes with time in patients with stroke, depending on age, stroke severity,

and other disabling diseases [1,35]. Our model revealed early improvement in urinary frequency, which may be due to the fact that the volume of cerebral infarcts by our method was smaller than that induced by the MCA occlusion method.

Once necrotic, mature neurons do not recover, but the urinary status of the rats changed after stroke in this study. It is possible that the surrounding tissue near the necrotic lesion, which is called the penumbra, compensated for the loss function. Microglia, the immune cells resident in the brain, are the first to respond to ischemic neurons and promote their survival [36]. Following this, it has been suggested that reactive astrocytes in the penumbra contribute to brain remodeling, such as neuronal circuitry and tissue reorganization [37]. Activations of these glial cells within the peri-infarct territory after focal cerebral infarction were reported to occur rapidly within a few days and were sustained for 14 days [38,39]. We suggest that the role of glial cells, such as microglia and astrocytes, has beneficial influence on the early improvement of dysuria in the PT model. Furthermore, complementation of function by structurally undamaged distant areas is a known mechanism of recovery after brain injury [37,40]. Other micturition centers, such as the insula, hypothalamus, and PAG, which have connections with PFC and ACC, may complement the voiding function [14,41].

Although this study has a limitation in that it is not directly comparable to the MCAO model, to the best of our knowledge, this is the first study to evaluate changes in the urinary status of rats after photothrombosis-induced cerebral infarction. Future studies should include more detailed investigations of changes in bladder tissue and local factors. We believe that this novel animal model, which reflects changes in voiding function as with clinical symptoms, may significantly contribute to development of new treatments for lower urinary tract dysfunction.

Conclusions

Our photothrombosis model was characterized by its simplicity, ability to create localized infarcts, nonlethal nature, and high reproducibility. Similar to the clinical course of a patient after stroke, this model observed changes in micturition status. In other words, this model would be suitable as a new model of urinary frequency caused by cerebral infarction.

Supporting information

S1 Fig. Photograph of the creation of photothrombosis. A: Identification of the bregma, the craniometric point at the junction of the sagittal and coronal sutures at the top of the cranium, marked with a black dot indicated by a yellow arrow. B: A fiber optic cable delivering a light source was fixed 1 mm anterior to the bregma on the midline under anesthesia inhalation. After Rose Bengal was injected, the skull was illuminated.

(TIF)

S2 Fig. All triphenyl tetrazolium chloride (TTC)-stained sagittal brain sections at Day 1. 2-mm slices of all brains in all sham and photothrombosis rats in the pilot study.

(TIF)

S1 File. Individual infarction volumes.

(XLSX)

S2 File. All individual data points of the modified neurological severity scores.

(XLSX)

S3 File. The raw cystometric data points used for preparing the figure graphs.

(XLSX)

Acknowledgments

The authors acknowledge the assistance of Naomi Kasuga in the experiments.

Author Contributions

Conceptualization: Yuya Ota, Yasue Kubota.

Formal analysis: Yuya Ota, Yuji Hotta, Taiki Kato.

Funding acquisition: Yuya Ota.

Investigation: Yuya Ota, Yuji Hotta, Nayuka Matsuyama, Taiki Kato, Takashi Hamakawa.

Methodology: Yuya Ota, Mami Matsumoto, Tomoya Kataoka.

Project administration: Yuya Ota, Yuji Hotta.

Resources: Nayuka Matsuyama, Taiki Kato, Takashi Hamakawa.

Software: Yuya Ota.

Supervision: Yasue Kubota, Kazunori Kimura, Kazunobu Sawamoto, Takahiro Yasui.

Validation: Yuji Hotta.

Writing – original draft: Yuya Ota.

Writing – review & editing: Yasue Kubota, Yuji Hotta, Kazunori Kimura, Kazunobu Sawamoto, Takahiro Yasui.

References

1. Sakakibara R, Hattori T, Yasuda K, Yamanishi T. Micturitional disturbance after acute hemispheric stroke: analysis of the lesion site by CT and MRI. *J Neurol Sci.* 1996; 137:47–56. [https://doi.org/10.1016/0022-510x\(95\)00322-s](https://doi.org/10.1016/0022-510x(95)00322-s) PMID: 9120487
2. Hannah P, Kim B, Park M, Hong J, Kim E. Effects of overactive bladder symptoms in stroke patients' health related quality of life and their performance scale. *Ann Rehabil Med.* 2017; 41:935–943. <https://doi.org/10.5535/arm.2017.41.6.935> PMID: 29354569
3. Zachariou A, Filiponi M, Kaltsas A, Dimitriadis F, Champilomatis I, Paliouras A, et al. Mirabegron alleviates the degree of burden experienced by caregivers of older females with mixed or urge incontinence: a prospective study. *Clin Interv Aging.* 2021; 16:291–299. <https://doi.org/10.2147/CIA.S283737> PMID: 33628016
4. Cardozo L, Amarenco G, Pushkar D, Mikulas J, Drogendijk T, Wright M, et al. Severity of overactive bladder symptoms and response to dose escalation in a randomized, double-blind trial of solifenacin (SUNRISE). *BJU Int.* 2013; 111:804–810. <https://doi.org/10.1111/j.1464-410X.2012.11654.x> PMID: 23294801
5. Yokoyama O, Ishiura Y, Komatsu K, Mita E, Nakamura Y, Kunimi K, et al. Effects of MK-801 on bladder overactivity in rats with cerebral infarction. *J Urol.* 1998; 159:571–576. [https://doi.org/10.1016/s0022-5347\(01\)63986-7](https://doi.org/10.1016/s0022-5347(01)63986-7) PMID: 9649294
6. Yokoyama O, Komatsu K, Ishiura Y, Nakamura Y, Morikawa K, Namiki M. Change in bladder contractility associated with bladder overactivity in rats with cerebral infarction. *J Urol.* 1998; 159:577–580. [https://doi.org/10.1016/s0022-5347\(01\)63987-9](https://doi.org/10.1016/s0022-5347(01)63987-9) PMID: 9649295
7. Longa EZ, Weinstein PR, Carlson S, Cummins R. Reversible middle cerebral artery occlusion without craniectomy in rats. *Stroke.* 1989; 20:84–91. <https://doi.org/10.1161/01.str.20.1.84> PMID: 2643202
8. Robert B, Nathalie K, Alexander K, Nerea F, Ana M, Pia Z, et al. FTY720 treatment in the convalescence period improves functional recovery and reduces reactive astrogliosis in photothrombotic stroke. *PLoS One.* 2013; 8:e70124. <https://doi.org/10.1371/journal.pone.0070124> PMID: 23936150
9. Yao H, Ago T, Kitazono T, Nabika T. NADPH oxidase-related pathophysiology in experimental models of stroke. *Int J Mol Sci.* 2017; 18:2123. <https://doi.org/10.3390/ijms18102123> PMID: 29019942
10. Watson BD, Dietrich WD, Busto R, Wachtel MS, Ginsberg MD. Induction of reproducible brain infarction by photochemically initiated thrombosis. *Ann Neurol.* 1985; 17:497–504. <https://doi.org/10.1002/ana.410170513> PMID: 4004172

11. Mares J, Nohejlova K, Stopka P, Rokyta R. Direct measurement of free radical levels in the brain after cortical ischemia induced by photothrombosis. *Physiol Res*. 2016; 65:853–860. <https://doi.org/10.33549/physiolres.933124> PMID: 27429112
12. Maria LC, Nanghong L, Jessica TG, James G, Maiken N. Direct comparison of microglial dynamics and inflammatory profile in photothrombotic and arterial occlusion evoked stroke. *Neuroscience*. 2017; 343:483–494. <https://doi.org/10.1016/j.neuroscience.2016.12.012> PMID: 28003156
13. Kuroiwa T, Guohua X, Ya H, Tavarekere NN, Joseph DF, Richard FK. Development of a rat model of photothrombotic ischemia and infarction within the caudoputamen. *Stroke*. 2009; 40:248–253. <https://doi.org/10.1161/STROKEAHA.108.527853> PMID: 19038913
14. Griffiths D, Tadic SD. Bladder control, urgency, and urge incontinence: evidence from functional brain imaging. *Neurourol Urodyn*. 2008; 27:466–474. <https://doi.org/10.1002/nau.20549> PMID: 18092336
15. Andrew J, Nathan PW. Lesions of the anterior frontal lobes and disturbances of micturition and defaecation. *Brain*. 1964; 87:233–262. <https://doi.org/10.1093/brain/87.2.233> PMID: 14188274
16. Yokoyama O, Ootsuka N, Komatsu K, Kodama K, Yotsuyanagi S, Niikura S, et al. Forebrain muscarinic control of micturition reflex in rats. *Neuropharmacology*. 2001; 41:629–638. [https://doi.org/10.1016/s0028-3908\(01\)00102-2](https://doi.org/10.1016/s0028-3908(01)00102-2) PMID: 11587718
17. Changfeng T, Jicheng W, Tao J, Ping W, Seong K, James R, et al. Brain switch for reflex micturition control detected by fMRI in rats. *J Neurophysiol*. 2009; 102:2719–2730. <https://doi.org/10.1152/jn.00700.2009> PMID: 19741099
18. Kuhtz JP, Gilster R, Horst C, Hamann M, Wolff S, Jansen O. Control of bladder sensations: an fMRI study of brain activity and effective connectivity. *Neuroimage*. 2009; 47:18–27. <https://doi.org/10.1016/j.neuroimage.2009.04.020> PMID: 19371782
19. Moskowitz MA, Lo EH, Iadecola C. The science of stroke: mechanisms in search of treatments. *Neuron*. 2010; 67:181–198. <https://doi.org/10.1016/j.neuron.2010.07.002> PMID: 20670828
20. Tsuyama J, Nakamura A, Ooboshi H, Yoshimura A, Shichita T. Pivotal role of innate myeloid cells in cerebral post-ischemic sterile inflammation. *Semin Immunopathol*. 2018; 40:523–538. <https://doi.org/10.1007/s00281-018-0707-8> PMID: 30206661
21. Angéla B, Krisztina M, Zsolt J, Gábor G, György L, László GH, et al. Use of TTC staining for the evaluation of tissue injury in the early phases of reperfusion after focal cerebral ischemia in rats. *Brain Res*. 2006; 1116:159–165. <https://doi.org/10.1016/j.brainres.2006.07.123> PMID: 16952339
22. Liu NW, Ke CC, Zhao Y, Chen YA, Chan KC, David TW, et al. Evolutional characterization of photochemically induced stroke in rats: a multimodality imaging and molecular biological study. *Transl Stroke Res*. 2017; 8:244–256. <https://doi.org/10.1007/s12975-016-0512-4> PMID: 27910074
23. Paxions G, Watson C. The rat brain in stereotaxic coordinates. 7th ed. San Diego: Academic Press; 2013.
24. Nagasaka Y, Yokoyama O, Komatsu K, Ishiura Y, Nakamura Y, Namiki M. Effects of opioid subtypes on detrusor overactivity in rats with cerebral infarction. *Int J Urol*. 2007; 14:226–231. <https://doi.org/10.1111/j.1442-2042.2007.01700.x> PMID: 17430260
25. Chen J, Li Y, Wang L, Zhang Z, Lu D, Lu M, et al. Therapeutic benefit of intravenous administration of bone marrow stromal cells after cerebral ischemia in rats. *Stroke*. 2001; 32:1005–1011. <https://doi.org/10.1161/01.str.32.4.1005> PMID: 11283404
26. Nasrin A, Akram E, Sakineh H, Siamak R, Hashim H. Effect of cerebrolysin on bladder function after spinal cord injury in female Wistar rats. *Int J Urol*. 2019; 26:917–923. <https://doi.org/10.1111/iju.14059> PMID: 31317583
27. Karl EA, Roberto S, Claudius F. Rodent models for urodynamic investigation. *Neurourol Urodyn*. 2011; 30:636–646. <https://doi.org/10.1002/nau.21108> PMID: 21661007
28. Hotta Y, Takahashi S, Tokoro M, Naiki-Ito A, Maeda K, Kawata R, et al. Anagliptin, a dipeptidyl peptidase-4 inhibitor, improved bladder function and hemodynamics in rats with bilateral internal iliac artery ligation. *Neurourol Urodyn*. 2020; 39:1922–1929. <https://doi.org/10.1002/nau.24449> PMID: 32725853
29. Luodan Y, Donovan T, Yan D, Chongyun W, Yujiao L, Yong L, et al. Photobiomodulation therapy promotes neurogenesis by improving post-stroke local microenvironment and stimulating neuroprogenitor cells. *Exp Neurol*. 2018; 299:86–96. <https://doi.org/10.1016/j.expneurol.2017.10.013> PMID: 29056360
30. Mohammad EA, Donovan T, Yan D, Yujiao L, Ningjun Z, Ruimin W, et al. Methylene Blue promotes cortical neurogenesis and ameliorates behavioral deficit after photothrombotic stroke in rats. *Neuroscience*. 2016; 336:39–48. <https://doi.org/10.1016/j.neuroscience.2016.08.036> PMID: 27590267
31. Felix F, Michael KS, Christoph K. Animal models of ischemic stroke and their application in clinical research. *Drug Des Devel Ther*. 2015; 9:3445–3454. <https://doi.org/10.2147/DDDT.S56071> PMID: 26170628

32. Kao YC, Li W, Lai HY, Oyarzabal EA, Lin W, Shih YY. Dynamic perfusion and diffusion MRI of cortical spreading depolarization in photothrombotic ischemia. *Neurobiol Dis.* 2014; 71:131–139. <https://doi.org/10.1016/j.nbd.2014.07.005> PMID: 25066776
33. Hosseini SM, Gholami PH, Naderi N, Sayyah M, Zibaii MI. Photothrombotically induced unilateral selective hippocampal ischemia in rat. *J Pharmacol Toxicol Methods.* 2018; 94:77–86. <https://doi.org/10.1016/j.vascn.2018.06.003> PMID: 29906509
34. Yokoyama O, Yoshiyama M, Namiki M, Groat WC. Role of the forebrain in bladder overactivity following cerebral infarction in the rat. *Exp Neurol.* 2000; 163:469–476. <https://doi.org/10.1006/exnr.2000.7391> PMID: 10833322
35. Nakayama H, Jørgensen HS, Pedersen PM, Raaschou HO, Olsen TS. Prevalence and risk factors of incontinence after stroke. The Copenhagen Stroke Study. *Stroke.* 1997; 28:58–62. <https://doi.org/10.1161/01.str.28.1.58> PMID: 8996489
36. Helena WM, Jessica AF. A quantitative spatiotemporal analysis of microglia morphology during ischemic stroke and reperfusion. *J Neuroinflammation.* 2013; 10:4. <https://doi.org/10.1186/1742-2094-10-4> PMID: 23311642
37. Murphy TH, Corbett D. Plasticity during stroke recovery: from synapse to behaviour. *Nat Rev Neurosci.* 2009; 10:861–872. <https://doi.org/10.1038/nrn2735> PMID: 19888284
38. Schroeter M, Schiene K, Kraemer M, Hagemann G, Weigel H, Eysel UT, et al. Astroglial responses in photochemically induced focal ischemia of the rat cortex. *Exp Brain Res.* 1995; 106:1–6. <https://doi.org/10.1007/BF00241351> PMID: 8542965
39. Li H, Zhang N, Lin HY, Yu Y, Cai QY, Ma L, et al. Histological, cellular and behavioral assessments of stroke outcomes after photothrombosis-induced ischemia in adult mice. *BMC Neurosci.* 2014; 15:58. <https://doi.org/10.1186/1471-2202-15-58> PMID: 24886391
40. Liepert J, Miltner WH, Bauder H, Sommer M, Dettmers C, Taub E, et al. Motor cortex plasticity during constraint-induced movement therapy in stroke patients. *Neurosci Lett.* 1998; 250:5–8. [https://doi.org/10.1016/s0304-3940\(98\)00386-3](https://doi.org/10.1016/s0304-3940(98)00386-3) PMID: 9696052
41. DasGupta R, Kavia RB, Fowler CJ. Cerebral mechanisms and voiding function. *BJU Int.* 2007; 99:731–734. <https://doi.org/10.1111/j.1464-410X.2007.06749.x> PMID: 17378838